Intraseasonal Oscillations and Interannual Variability of the Indian Summer Monsoon

B. N. GOSWAMI AND R. S. AJAYA MOHAN

Centre for Atmospheric and Oceanic Sciences, Indian Institute of Science, Bangalore, India

(Manuscript received 6 May 1999, in final form 1 May 2000)

ABSTRACT

How and to what extent the intraseasonal oscillations (ISOs) influence the seasonal mean and its interannual variability of the Indian summer monsoon is investigated using 42-yr (1956–97) daily circulation data from National Centers for Environmental Prediction–National Center for Atmospheric Research 40-Year Reanalysis and satellite-derived outgoing longwave radiation data for the period of 1974–97. Based on zonal winds at 850 hPa over the Bay of Bengal, a criterion is devised to define ''active'' and ''break'' monsoon conditions. The underlying spatial structure of a typical ISO cycle in circulation and convection that is invariant over the years is constructed using a composite technique. A typical ISO has large-scale horizontal structure similar to the seasonal mean and intensifies (weakens) the mean flow during its active (break) phase. A typical active (break) phase is also associated with enhanced (decreased) cyclonic low-level vorticity and convection and anomalous upward (downward) motion in the northern position of the tropical convergence zone (TCZ) and decreased (increased) convection and anomalous downward (upward) motion in the southern position of the TCZ. The cycle evolves with a northward propagation of the TCZ and convection from the southern to the northern position of the TCZ.

It is shown that the intraseasonal and interannual variations are governed by a common mode of spatial variability. The spatial pattern of standard deviation of intraseasonal and interannual variability of low-level vorticity is shown to be similar. The spatial pattern of the dominant mode of ISO variability of the low-level winds is also shown to be similar to that of the interannual variability of the seasonal mean winds. The similarity between the spatial patterns of the two variabilities indicates that higher frequency of occurrence of active (break) conditions would result in ''stronger'' (''weaker'') than normal seasonal mean. This possibility is tested by calculating the two-dimensional probability density function (PDF) of the ISO activity in the low-level vorticity. The PDF estimates for ''strong'' and ''weak'' monsoon years are shown to be asymmetric in both the cases. It is seen that the strong (weak) monsoon years are associated with higher probability of occurrence of active (break) conditions. This result is further supported by the calculation of PDF of ISO activity from combined vorticity and outgoing longwave radiation. This clear signal indicates that the frequency of intraseasonal pattern determines the seasonal mean. Because the ISOs are essentially chaotic, it raises an important question on predictability of the Indian summer monsoon.

1. Introduction

The Indian summer monsoon has vigorous intraseasonal oscillations in the form of ''active'' and weak (or ''break'') spells of monsoon rainfall within the summer monsoon season (Ramamurthy 1969). These ''active and break spells of the monsoon are associated with fluctuations of the tropical convergence zone (TCZ; Yasunari 1979, 1980, 1981; Sikka and Gadgil 1980). The TCZ over the Indian monsoon region represents the ascending branch of the regional Hadley circulation. These fluctuations initially seen in Indian station data (Keshavamurthy 1973; Dakshinamurthy and Keshavamurthy 1976) were later shown to be related to coherent fluctuations of the regional Hadley circulation (Krishnamurti and Subramaniam 1982; Murakami et al. 1984; Mehta and Krishnamurti 1988; Hartman and Mitchelson 1989). The intraseasonal oscillations (ISOs) of the Indian summer monsoon represent a broadband spectrum with periods between 10 and 90 days but have two preferred bands of periods (Krishnamurti and Bhalme 1976; Krishnamurti and Ardunay 1980; Yasunari 1980), one between 10 and 20 days and the other between 30 and 60 days.

Several recent modeling studies show that a significant fraction of the interannual variability of the seasonal mean Indian summer monsoon is governed by internal chaotic dynamics (Goswami 1998; Hazrallah and Sadourny 1995; Rowell et al. 1995; Stern and Miyakoda 1995). Most of these studies, however, do not provide any insight regarding the origin of the internally generated interannual variability. The monsoonal ISOs are known to be governed by internal dynamics (Web-

Corresponding author address: Dr. B. N. Goswami, Centre for Atmospheric and Oceanic Sciences, Indian Institute of Science, Bangalore 560 012, India.
E-mail: goswamy@caos.iisc.ernet.in

ster 1983; Goswami and Shukla 1984; Keshavamurthy et al. 1986). Because the separation between the dominant ISO periods and the season is not large, the statistics of the ISOs could, in principle, influence the seasonal mean monsoon and its interannual variability. Based on a series of sensitivity studies with an atmospheric GCM and a dynamical system model, Goswami (1997) shows that modulation of the ISOs by the annual cycle could give rise to an internal quasi-biennial oscillation in the tropical atmosphere and influence the interannual variability of the Indian monsoon. To the extent that the ISOs are intrinsically chaotic and unpredictable, the predictability of the Indian summer monsoon would depend on relative contribution of the ISOs to the seasonal mean compared to the externally forced component.

Unfortunately, how and to what extent the ISOs influence the seasonal mean circulation and precipitation has not been clearly established. Not many studies have actually addressed this question. Mehta and Krishnamurti (1988) examined the interannual variability of the 30–50 day mode with the winds at 850 and 200 hPa for the period 1980–84 using the European Center for Medium Range Weather Forecasts (ECMWF) operational analysis. They mainly examined the variations in the northward propagation characteristics and did not attempt to relate these to the seasonal mean. Singh and Kripalani (1990) and Singh et al. (1992) used long records of daily rainfall data over the Indian continent and examined the 30–50 day oscillation. They, however, could not come to a clear conclusion regarding relationship between the ISOs and the interannual variability of the Indian monsoon rainfall. Ahlquist et al. (1990) studied radiosonde observations at 12 Indian stations between 1951 and 1978 and examined ISOs with periods longer than 10 days but did not try to relate the ISOs with the interannual variability of the monsoon. Using simulations of the Indian monsoon for 1988 and 1987 by a GCM, Fennessy and Shukla (1994) showed that the spatial structures of the interannual variability and the intraseasonal variability are quite similar. Ferranti et al. (1997) studied the relationship between intraseasonal and interannual variability over the monsoon region using data from five 10-yr simulations of the ECMWF GCM differing only in their initial conditions. They showed that monsoon fluctuations within a season and between different years have a common mode of variability with a bimodal meridional structure in the precipitation. However, their results suffer from some systematic errors inherent in the ECMWF GCM simulation of the Indian summer monsoon. The model underestimates precipitation over the north Bay of Bengal and the monsoon trough zone. This systematic error reflects in their interannual mode, having appreciable amplitude only east of 80°E both in precipitation and low-level vorticity. Webster et al. (1998) discusses the mean circulation pattern at 850 hPa associated with active and break conditions based on ECMWF operational analysis for 14 yr (1980–93) and brings out the large-scale nature of these circulation anomalies. No attempt to relate these patterns to the seasonal mean was, however, made. In another recent study, Goswami et al. (1998) studied daily surface winds from National Centers for Environmental Prediction–National Center for Atmospheric Research (NCEP–NCAR) 40-Year Reanalysis for 10 yr (1987–96), showed that the spatial structures of the intraseasonal mode and that of the dominant interannual mode are similar, and made a start in relating the ISOs with the interannual variability from observations. Recently, Annamalai et al. (1999) examined the relationship between the intraseasonal oscillations and interannual variability using NCEP–NCAR reanalysis and ECMWF reanalysis for the period 1979–95. Unlike the results of some earlier model studies, they concluded that there was not a common mode that described intraseasonal and interannual variability. However, because of small sample size, the statistical significance of their result could not be ascertained.

A conceptual model of how the ISOs influence the seasonal mean and interannual variability of the Indian monsoon was proposed by Goswami (1994). The conceptual model is based on the similarity between the spatial structure of the dominant ISO mode and that of the interannual variability. The seasonal summer mean (June–September, JJAS) precipitation distribution has a major zone of large precipitation along the monsoon trough extending to the north Bay of Bengal (see Fig. 1d) and a secondary zone of precipitation maximum south of the equator (between 0° and 10°S) over the warm waters of the Indian Ocean. These two maxima in the seasonal mean precipitation represent two favored locations of the TCZ during the summer monsoon season (Sikka and Gadgil 1980; Goswami 1994). The ISOs are fluctuations of the TCZ between the two locations and repeated propagation from the southern to the northern position within the monsoon season. During a typical active condition, the northern TCZ is stronger and the southern one is weaker, with stronger cyclonic vorticity and enhanced convection over the northern location and stronger anticylonic vorticity and decreased convection over the southern one. The situation reverses during a typical break condition. Higher probability of occurrence of activelike (breaklike) conditions during a monsoon season could, therefore, give rise to stronger (weaker) than normal seasonal mean monsoon and precipitation. It may be noted that the ISOs are not purely sinusoidal oscillations. Because of the broadband nature of their spectrum, the intensity as well as the duration of the active phases in a season could be different from those of the break phases. Moreover, the number of active and break spells within a monsoon season (1 June–30 September) may be different depending on the initial phase. These factors may lead to asymmetry in the probability density functions (PDF). Our conceptual model is similar to the one proposed by Palmer (1994). However, in contrast to Palmer (1994), who proposes

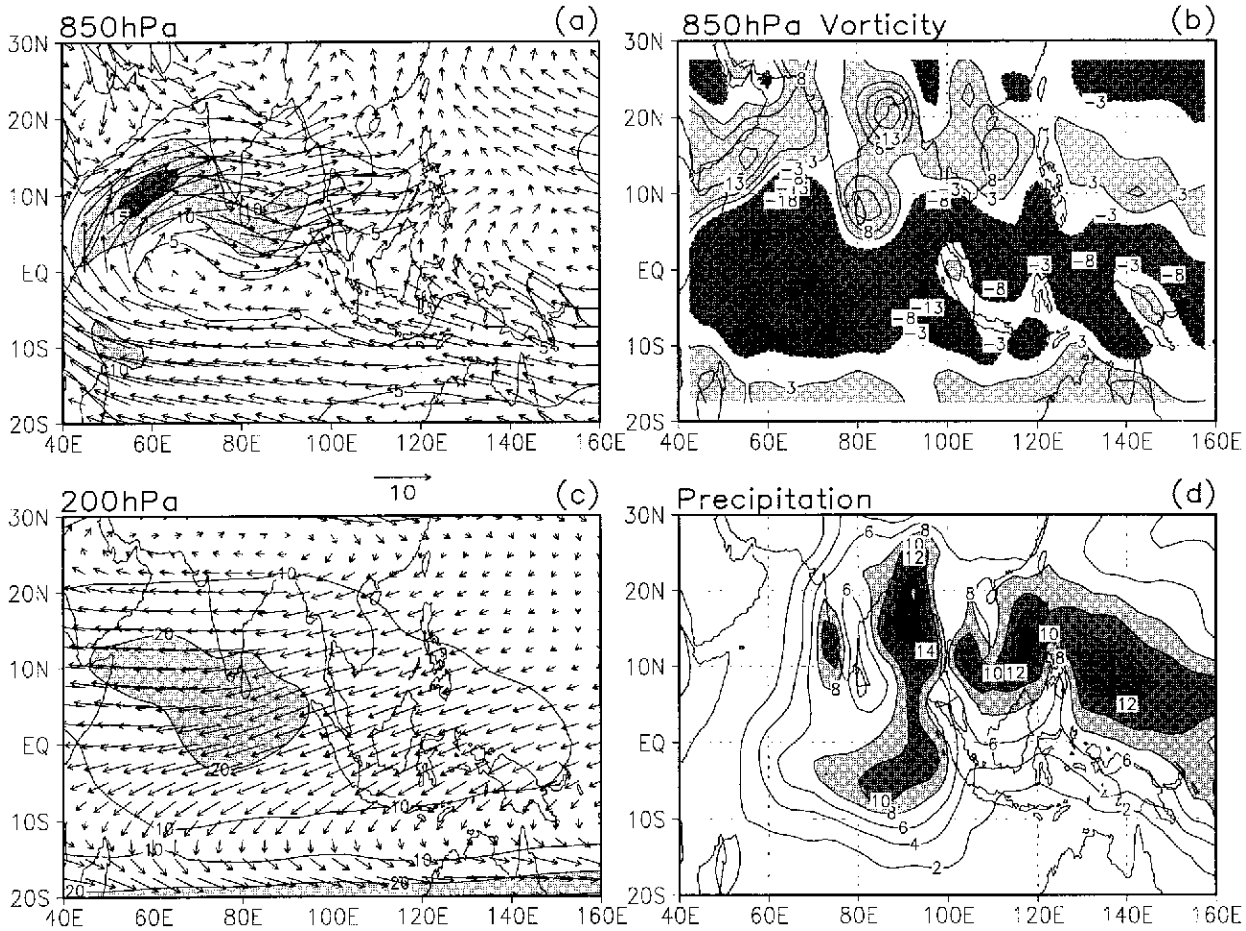

FIG. 1. Climatological mean (JJAS) monsoon winds (m s^{-1}) and precipitation (mm day^{-1}): (a) 850-hPa vector winds; (b) relative vorticity at 850 hPa (10^{-6} s^{-1}); (c) 200-hPa vector winds, contour interval for isotachs at 850 hPa is 5 m s^{-1}, that for 200 hPa is 10 m s^{-1}; (d) JJAS precipitation from Xie and Arkin (1996). Contours greater than 8 mm day^{-1} are shaded.

that the asymmetry in the PDF is forced only by external forcing, we claim that the asymmetry could arise even without external forcing.

The primary objective of the present study is to examine sufficiently long daily observations to bring out how and to what extent the ISOs of the Indian monsoon affect the seasonal mean and its interannual variability. We use the conceptual model proposed above as the working hypothesis. The primary objective may be achieved in two parts. First, we bring out the underlying common spatial structure of the dominant ISO in all years and compare it with the spatial structure of the seasonal mean and interannual variability of the Indian monsoon. Second, an attempt is made to relate probability of occurrence of the ISO pattern to the interannual variability of the seasonal mean. To achieve this goal, we need a homogeneous dataset for a long enough period so that the statistics of the ISOs and that of the interannual variability of the seasonal mean could be accurately estimated. Many earlier studies used data only for a short period which resulted in the inaccurate estimate of the interannual variability of the circulation. Results of some other earlier studies that used operational analysis were contaminated by artificial jumps introduced by changes in the operational analysis system. In this study, we use daily circulation data at several vertical levels from the NCEP–NCAR reanalysis project (Kalnay et al. 1996) for a 42-yr period (1956–97). We also use observed daily outgoing longwave radiation (OLR) for the period 1974–97 to derive insight regarding the dynamics of the ISOs. The datasets used are described in section 2. The general characteristics of the ISOs are described in section 3. A criterion for defining active and break monsoon conditions based on a circulation index is proposed in section 3a. The climatological mean structure of the ISOs is described in section 3b. The relationship between the ISOs and the interannual variability of the monsoon is discussed in section 4. The main results are summarized in section 5.

2. Datasets used and some elements of analysis

The study uses daily averaged zonal (u) and meridional (v) components of winds at surface, 850, 500, and

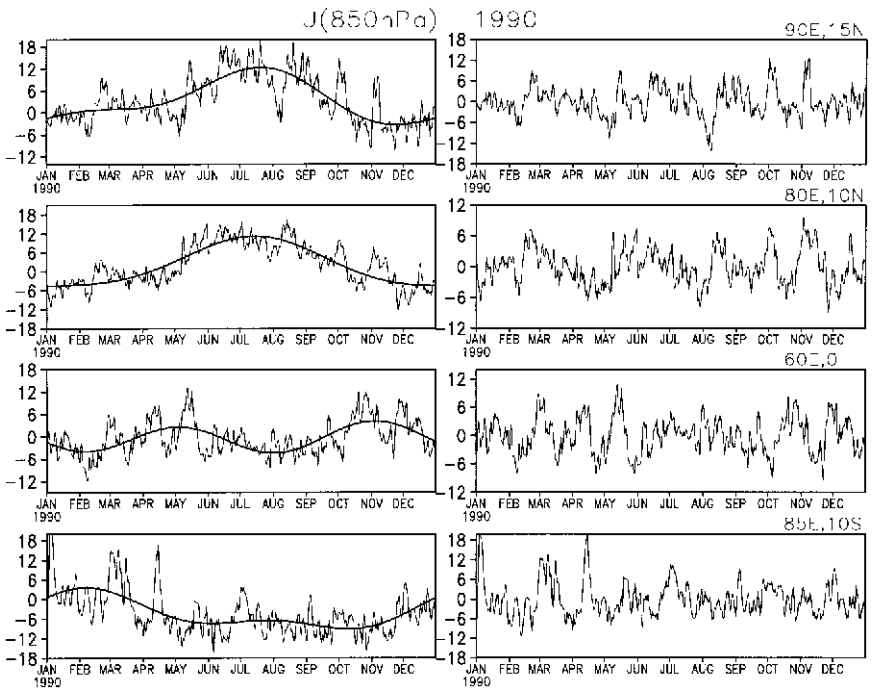

FIG. 2. Some examples of raw time series of zonal winds at 850 hPa at a few selected points during 1990. (left) Daily zonal winds (m s^{-1}) with the annual cycle (annual and semiannual harmonics, thick lines). (right) Anomalous daily zonal winds (m s^{-1}).

200 hPa from the NCEP–NCAR reanalysis project for the period of 1956–97. The NCEP–NCAR reanalysis project uses a frozen state-of-the-art analysis system (the Global Data Assimilation System, GDAS) and a forecast model with T63 horizontal resolution and a database as complete as possible (Kalnay et al. 1996). Because of the fact that the analysis system and the forecast model are kept unchanged throughout the period of reanalysis, the reanalysis data is expected to be devoid of artificial climate jumps. To accurately estimate the interannual variability, we have also used monthly mean wind at the same levels from the same reanalysis for 40 yr (1958–97). To study the relationship between circulation and convection, daily satellite-derived OLR data are also used (Gruber and Krueger 1984; Salby et al. 1991) for the period of 1974–97. The OLR data contain a major data gap of several months during 1978 due to the failure of the satellite. The circulation data as well as the OLR data are at 2.5° × 2.5° latitude–longitude resolution. We use All India Monsoon Rainfall (IMR) index as defined by Parthasarathy et al. (1994) for categorizing ''strong'' and ''weak'' monsoons. Daily gridded rainfall over the Indian continent for 12 yr (1978–89) will also be utilized. The daily rainfall data was originally compiled by Singh et al. (1992) at 2.5° lat × 2.5° long boxes based on daily rainfall at 365 stations distributed uniformly over the country. The original data reported in Singh et al. (1992) were later extended to 1989. The version we use was regridded to 1.25° lat × 1.25° long boxes by M. Fennessy of the Center for Ocean–Land–Atmosphere Studies (COLA) (1999, personal communication). The gridded rainfall data for the recent years are not yet available to us.

The circulation, convection, and precipitation in the monsoon region are characterized by a strong seasonal cycle. An example of zonal winds at 850 hPa at a few selected points for 1990 is shown in Fig. 2. The annual cycle is defined by the sum of the annual and semiannual harmonics (thick solid lines in Fig. 2). The daily anomalies after removing the annual cycle are shown in the right panel. The annual cycle, which is essentially driven by external conditions, has year-to-year variations that manifest in the interannual variations of the seasonal mean. In many studies, daily anomalies are constructed by removing the climatological mean for each day from the daily observations. In a particular year, the annual cycle may be significantly different from the climatological mean annual cycle. This would introduce an additional bias in the daily anomalies during the monsoon season. This bias can give rise to asymmetry in the PDF of the ISOs that may not be intrinsic to the ISOs but may be related to the external forcing changes. Since we are interested in the role of ISOs in modifying the summer mean, we would like to avoid aliasing of any statistics of the ISOs due to possible year-to-year variation of the annual cycle itself. This is achieved by calculating the annual cycle for each year based on the data for that year alone and by calculating the daily anomalies after removing the annual cycle of each year.

The intraseasonal oscillations are identified by esti-

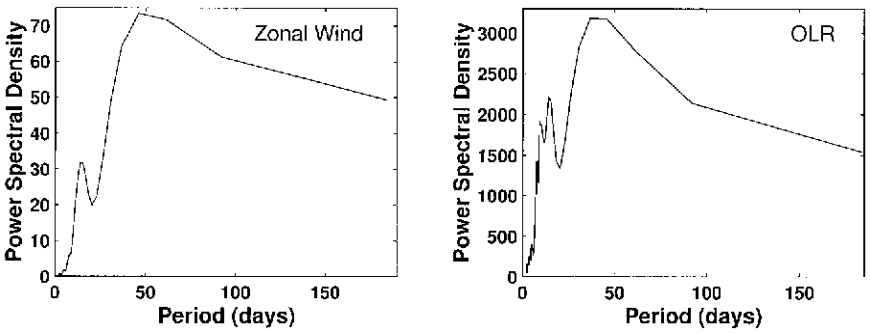

FIG. 3. Examples of spectra of zonal winds and OLR for a typical year (1984) at a typical point (90°E, 10°N).

mating the spectra of zonal and meridional winds as well as OLR anomalies. Power spectra are calculated from anomaly time series between 1 May and 31 October (184 days) using the Tukey lag window method (Chatfield 1980). An example of spectra for zonal winds and OLR at a point in north Bay of Bengal for 1984 is shown in Fig. 3. This example shows two strong peaks, one with period around 42 days and the other with period around 16 days. Similar power spectral estimates are made for each year and at all latitudes between 30°S and 30°N along a number of longitudes (e.g., 70°, 80°, 90°E). From these estimates, the most prevalent dominant periods are chosen. It is also found that the dominant periods found from the winds agree well with those found from OLR. The dominant periods found in each year of the 20-yr period (1978–97) are listed in Table 1. To study the detailed structure and characteristics of the two (ISOs) Butterworth bandpass filters with peak response around the dominant periods are used (Murakami 1979).

Different lengths of data are used for fulfilling different objectives. To obtain the mean spatial pattern common to all episodes of the dominant ISO variability, we use 20-yr data of circulation and OLR (1978–97). This includes calculation of composite structure, intraseasonal empirical orthogonal function (EOF), and so on. However, to study the role of the ISOs on interannual variability, we use a longer dataset. In particular, to calculate the PDF of ISO activity during the strong and weak Indian monsoon, 42-yr daily circulation data (1956–97) is used. This period includes 7 strong monsoon years (as defined by IMR $>$ 1 std dev) and 10 weak years (IMR $<$ 1 std dev). However, to calculate PDF of ISOs of combined circulation and OLR, we could use only a 24-yr dataset because the OLR is available only from 1974.

TABLE 1. Periods in days corresponding to the two peaks in the spectra for different years.

Year	Mode I	Mode II
1978	25	12
1979	42	17
1980	33	13
1981	42	16
1982	42	14
1983	25	14
1984	42	16
1985	33	12
1986	42	12
1987	30	10
1988	42	20
1989	40	14
1990	42	16
1991	42	20
1992	34	14
1993	32	14
1995	42	20
1994	30	12
1996	32	12
1997	42	12

3. Intraseasonal oscillations

The characteristics of the monsoonal ISOs, such as their horizontal and vertical structures and meridional and zonal propagation characteristics, have previously been studied extensively. Our objective here is not to repeat the results of the earlier studies. However, earlier studies (cited in the introduction) used limited numbers of years. As a result, it is not well established whether different phases of the dominant ISO mode possess spatial patterns that are common to all events. Our aim here is to bring out the underlying mean feature of the dominant ISO mode that is invariant over the years. First, some known results are briefly summarized. The 30–60-day mode has a large horizontal scale (half wavelength of 70°–80° longitude), as seen from the point-correlation map of the 30–60-day filtered zonal winds with respect to those at a reference point (Fig. 4a). The mode has a first baroclinic vertical structure close to the equator and over the Indian monsoon region, as seen from correlations between 30–60-day filtered zonal winds at 850 and 200 hPa (Fig. 4b). The horizontal scale and vertical structure of the mode, shown in the example (Fig. 4), is representative of other years. The 30–60-day mode is known to have a northward and eastward propagation in the Indian monsoon region (Yasunari 1979, 1980). The 10–20-day mode, on the average, has

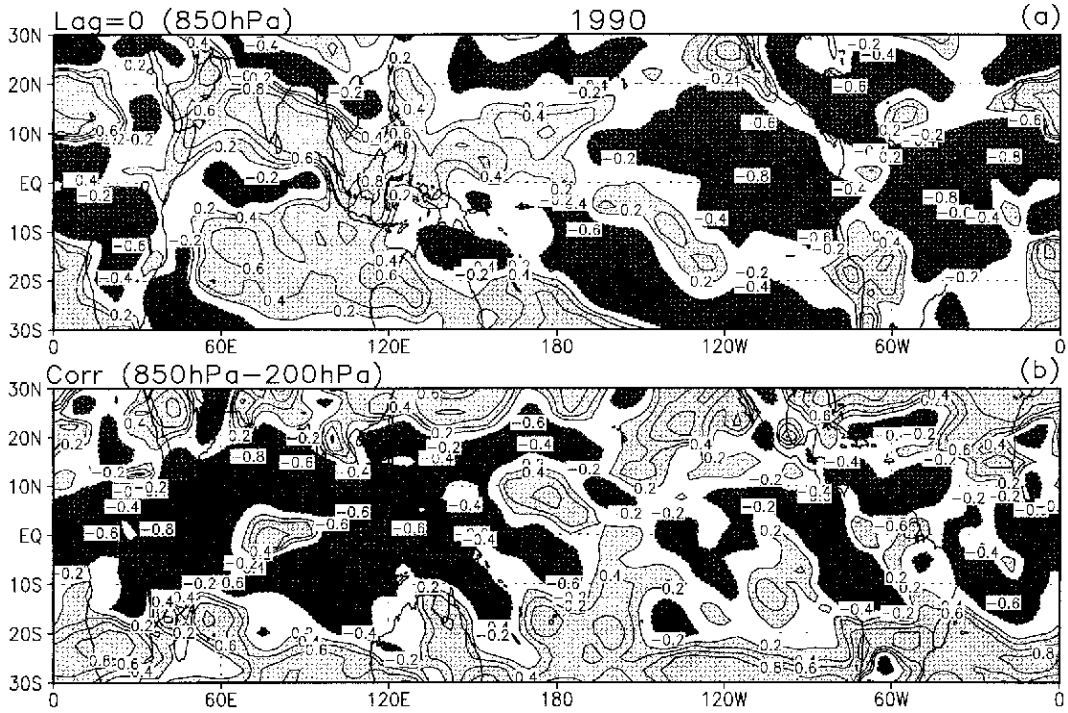

FIG. 4. An example illustrating the horizontal scale and vertical structure of the dominant ISO mode. (a) Lag-zero correlations of the 850-hPa, 30–60-day filtered zonal winds with respect to a reference point (85°E, 10°N); (b) lag-zero correlations between 30–60-day filtered zonal winds at 850 and 200 hPa at each grid point. Correlations are calculated between 1 May and 31 Oct 1990. Correlations exceeding 0.2 are significant at 95% confidence level.

clear westward propagation in the monsoon region. It is either stationary or northward propagating in the meridional direction (figures not shown).

a. A circulation criterion for active and break monsoon conditions

Active and break monsoon conditions are traditionally defined based on a precipitation criterion (Ramamurthy 1969). Here, we propose a criterion to define active and break monsoon conditions based on a circulation index. Such a circulation-based definition of active and break monsoons may be useful for various purposes. During an active phase of the Indian monsoon, typically there is more precipitation over central India and a stronger monsoon trough (Ramamurthy 1969). As a result, we may expect westerly zonal winds south of the monsoon trough to strengthen. The opposite is expected during a break phase. With this consideration in mind, we propose a circulation-based definition of active and break monsoon conditions. A reference point just south of the ''monsoon trough'' (90°E, 15°N) is selected for this purpose and the 30–60-day filtered zonal winds at 850 hPa are plotted (Fig. 5a). The days for which the filtered zonal winds at 850 hPa are greater than +1 standard deviation (as shown by the thin solid line, i.e., stronger westerly anomalies) are considered active days, while those less than −1 standard deviation (i.e., stronger easterly anomalies) are considered break days. The method of defining active and break conditions is somewhat similar to the one used by Webster et al. (1998), where they also used a zonal wind criterion over the north Bay of Bengal but used a fixed cutoff anomaly (+3 m s^{-1} or −3 m s^{-1}) to define active and break conditions. Our method of defining active and break is also similar to the one used by Krishnamurti and Subramaniam (1982) for the year 1979, where they used filtered zonal wind at a point in the Arabian Sea to define active and break episodes. The identification of the active and break days is not very sensitive to small changes in the position of the reference point. We note that between 1 June and 30 September of this particular year, there were two active and three break episodes. The active and break days are thus identified for all years.

To test whether our criterion for defining active and break monsoon conditions is related to the traditional, precipitation-based criterion, we calculated daily precipitation composites for all active and break days defined by the circulation criterion for the period of 1978–89 from 1 June to 30 September. The precipitation difference between active and break composites is shown in Fig. 5b. It is clear that the pattern of precipitation anomalies during active (break) conditions is identical to the dominant EOF of daily (or pentad) rainfall (Singh and Kripalani 1990; Krishnamurthy and Shukla 2000),

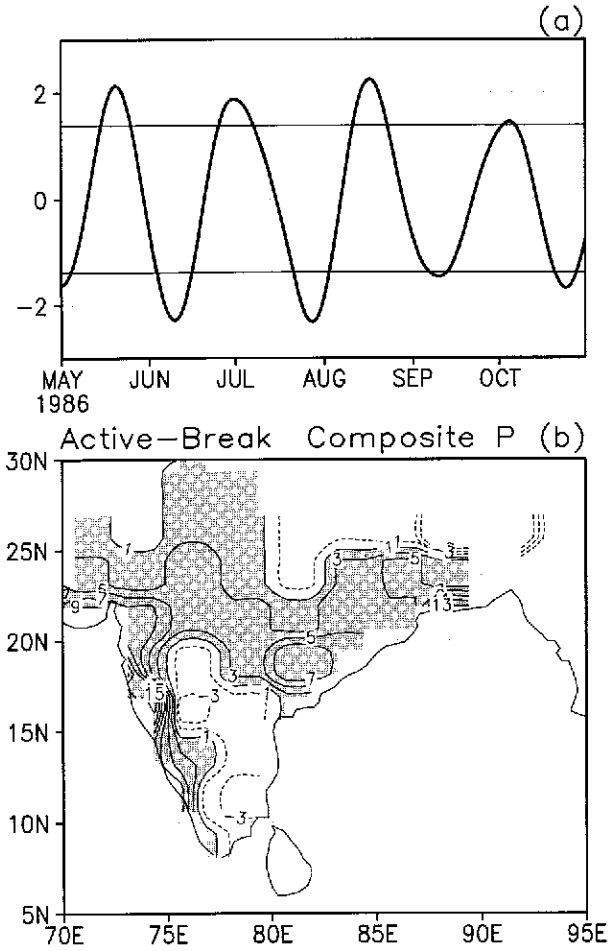

FIG. 5. (a) An example of 30–60-day filtered zonal winds for 1985 at a reference point (15°N, 90°E). The thin horizontal lines correspond to +1 and −1 std dev. Active break days are defined as days for which the filtered zonal winds at the reference point are greater than +1 std dev (or less than −1 std dev). (b) 12-yr (1978–89) mean precipitation difference (mm day^{-1}) between all active and break composites. Contours are ±1, 3, 5, 7, 9, 11, 13, and 15.

with an active monsoon condition being associated with enhancement of precipitation over most of continental India except a small region in southeastern India and another in the northeastern corner. Thus, the active and break monsoon conditions defined by our circulation criterion captures the dominant mode of intraseasonal precipitation variability over the Indian continent and hence are essentially same as those defined by traditional precipitation criterion.

As the low-level jet over Somali is also usually strengthened (weakened) during an active (break) condition, one could also select a reference point in the Arabian Sea (e.g., 60°E, 10°N) and 850 hPa zonal wind to define the ISOs.

b. Mean structure of the ISOs

In this section, we isolate the underlying common spatial patterns associated with different phases of the dominant ISO modes. The phase composite technique (Murakami and Nakazawa 1985; Murakami et al. 1984) is followed to illustrate the common mode of evolution of the oscillations. Having defined the active and break days, as described in section 3a, averaged vector wind anomalies at 850 hPa associated with all the active and break phases of the 30–60-day mode are calculated within a year. A climatological mean composite active phase constructed by averaging active composites of 20 yr is shown in Fig. 6a together with the associated composite relative vorticity pattern. The composite of all break phases is also shown in Fig. 6a. The significant coherent large-wind anomalies, which emerge after averaging over about 80 active (break) episodes over a period of 20 yr, shows that all active (break) phases possess a common spatial pattern of variability. The other important feature that emerges from the composite is the large zonal scale of the circulation changes associated with active (break) phases of the Indian monsoon extending from about 50° to 120°E. During the active phase, the mean monsoon circulation is strengthened, and the monsoon trough cyclonic vorticity is enhanced north of 10°N (compare with Figs. 1a,b). The anticyclonic vorticity is enhanced between the equator and 10°N, and cyclonic vorticity is weakened in the Southern Hemisphere. The mean composite 850 hPa wind anomalies corresponding to active and break conditions (Fig. 6a) is consistent with the pattern shown in Webster et al. (1998). The climatological mean composite active and break phase vector wind anomalies at 500 and 200 hPa are shown in figure in Fig. 6b. At 500 hPa during active phase, the vector wind anomalies bear close resemblance with those at 850 hPa, with cross-equatorial flow and enhancement of monsoon trough vorticity. At 200 hPa, the vorticity anomalies over the monsoon trough have become anticyclonic, and the equatorial wind anomalies are generally out of phase with those at 850 hPa, consistent with a first baroclinic mode vertical structure for this mode.

The composite picture of active and break conditions described above is consistent with a seesaw between the two favorable positions of the TCZ, as mentioned in the introduction. If this scenario is correct, there should be enhanced convection in the northern position and decreased convection in the southern position during an active phase, while it should be the other way round during a break phase. Figure 7 supports this conjecture that the composite of unfiltered OLR anomalies for all active and break days are plotted. The active and break days used in the composite are exactly the same days defined by the 30–60-day zonal winds at the reference point as in the circulation composite. Coherence of the OLR anomalies averaged over 20 yr of active and break conditions defined by the circulation criterion shows that there is a close relationship between circulation and convection associated with active and break conditions. A notable feature of the composites is the meridional seesaw of the convection anomalies consistent with the

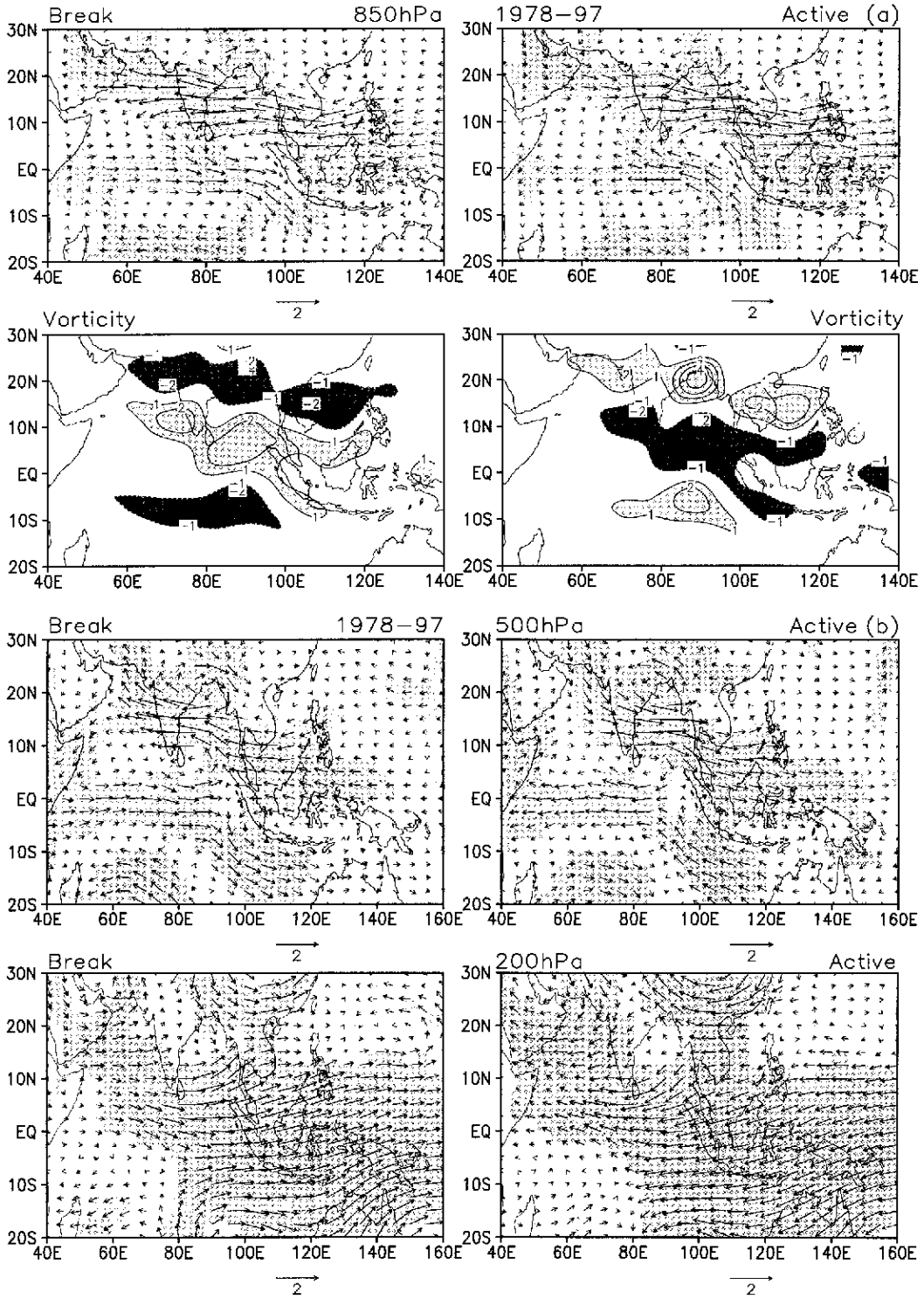

FIG. 6. (a) Climatological mean composite vector wind anomalies (m s^{-1}) at 850 hPa corresponding to active and break conditions for the 30–60-day mode (upper) and associated relative vorticity (10^{-6} s^{-1}; lower). The climatological mean composite is calculated by averaging all active and break conditions occurring during the 20-yr period (1978–97). Shading in the upper panels indicates regions with anomalies significant above 90% confidence level. (b) Same as Fig. 6a but for wind anomalies (m s^{-1}) at 500 hPa (upper) and at 200 hPa (lower).

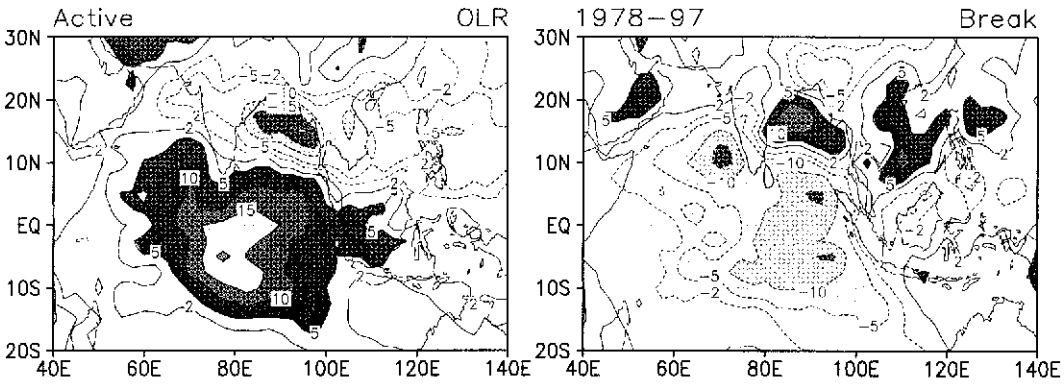

FIG. 7. Climatological mean composite OLR anomalies (W m^{-2}) corresponding to active and break conditions. Active and break composites are constructed using unfiltered OLR anomalies and the same active and break dates defined by 30–60-day filtered zonal wind anomalies as used in Fig. 6a. OLR anomalies above 5 W m^{-2} are significant above 90% confidence level.

low-level vorticity anomalies. It is also worth noting that even after averaging over approximately 80 active (break) episodes, fluctuations of OLR anomalies up to ± 15 W m^{-2} is seen over the two preferred regions. This means that, notwithstanding some variation in the intensity and mean position of the TCZ from one active (break) episode to another, there exists a common mean position of the TCZ during a typical active (break) episode. During individual years, it is not unusual to see ± 25 W m^{-2} OLR anomalies over either of the zones. To put the dynamical link between low-level cyclonic vorticity and convection on a stronger footing, climatological mean composites of unfiltered pressure vertical velocity (ω) anomalies at 500 hPa corresponding to the same active and break days over the full 20-yr period were also constructed. It is seen that (figure not shown) enhanced (decreased) convection shown in Fig. 7 is clearly associated with upward (downward) motion in both active and break conditions. Location and spatial pattern of the vertical velocity anomalies correspond well with those of the convection anomalies. Thus, active (break) conditions are associated with a seesaw of the anomalous regional Hadley circulation. We have also studied the evolutionary cycle of the mode by constructing composites of vector wind and OLR anomalies corresponding to eight different phases of the oscillation (figures not shown). In addition to showing clear northward propagation of the ISO, a strong relationship between low-level vorticity and OLR is seen through the evolutionary cycle.

The active and break composites are constructed for the 10–20-day mode following a similar procedure. Active (Break) conditions are now defined by the 10–20-day filtered zonal winds at 850 hPa being greater than $+1$ standard deviation (less than -1 std dev) at the same reference point south of the monsoon trough. Due to its shorter period, it is possible to have 8–10 episodes of active or break conditions for this mode during the summer monsoon season. The climatological mean active (break) composite vector wind anomalies for the 10–20-day mode based on the entire 20-yr period at 850 hPa is shown in Fig. 8 together with the corresponding relative vorticity. The most important feature of this mode is that it has a much smaller horizontal scale, confined mainly to the Bay of Bengal. Active (Break) conditions are associated with a strong cyclonic (anticyclonic) vortex at the north Bay of Bengal, with an anticyclonic (cylconic) vortex south of it between 10°N and the equator. Because of the localized character of the 10–20-day mode, it is unlikely to have a strong influence on the large-scale mean circulation. However, depending on the phase relationship between the two ISOs, the strong cyclonic (anticyclonic) vorticity over the north Bay of Bengal associated with the active (break) phase of the 10–20-day mode can enhance (weaken) the cyclonic vorticity over the monsoon trough zone associated with the 30–60-day mode (Goswami et al. 1998). In this manner, it can indirectly contribute to the mean monsoon circulation.

4. ISOs and interannual variability

In order to include the effect of both the ISO modes and keeping in mind their interannual variations in their peak period, total intraseasonal activity is defined by a bandpass filtered field with peak response at 35 days and half responses at 15 days and 80 days, respectively. For all the calculations described below, these ISO-filtered fields are used to bring out the relationship between ISO and interannual variability.

a. A common mode of intraseasonal and interannual variability

In section 3b, we have shown that the large-scale structure of the wind associated with the dominant ISO mode is quite similar to that of the seasonal mean wind, strengthening and weakening the large-scale flow during

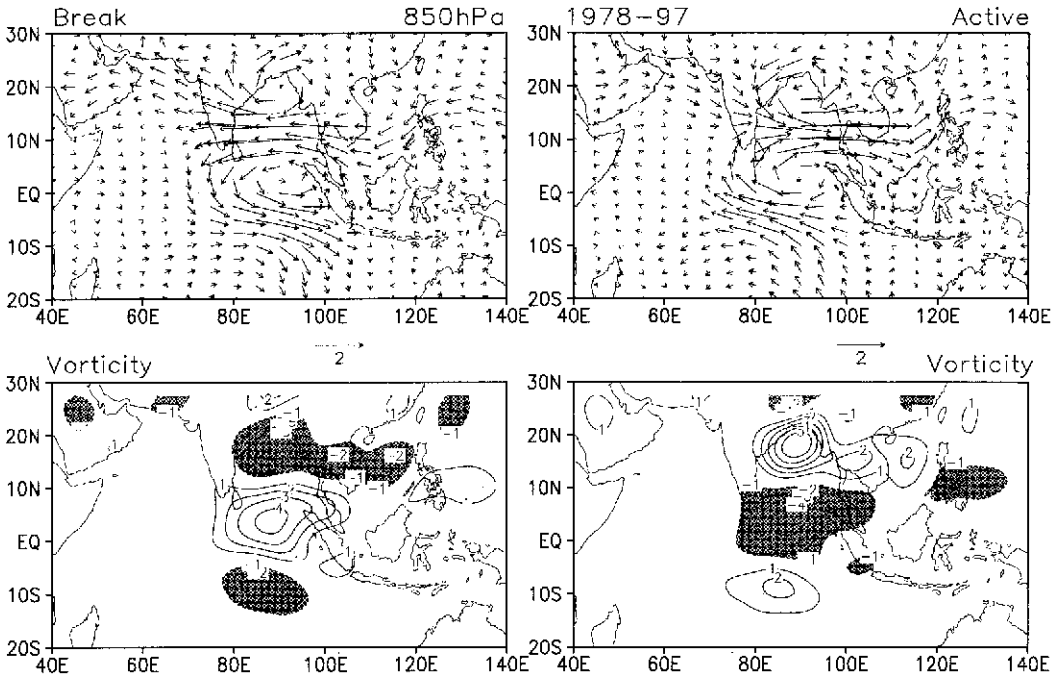

FIG. 8. Same as Fig. 6a but for the 10–20-day mode using 10–20-day filtered winds.

its active and break phases, respectively. This similarity between the structure of the intraseasonal variability and the seasonal mean flow provides the basis for our hypothesis that the ISOs could influence the seasonal mean and its interannual variability. In this section, we provide further evidence that the spatial structure of the intraseasonal variability and the interannual variability are similar. The geographical distribution of the intraseasonal activity and the interannual variability are compared in Fig. 9. In this figure, the standard deviation of ISO-filtered 850-hPa relative vorticity averaged over the 20-yr period (1978–97) and interannual standard deviation of the seasonal mean (JJAS) relative vorticity based on the same 20-yr period are shown. The similarity of the geographical distribution of intraseasonal variability and interannual variability of 850-hPa relative vorticity is noteworthy. The correlation between the two patterns is 0.6. Both patterns are characterized by strong activity in the two favored positions of the TCZ, namely a northern position around the monsoon trough and a southern position between the equator and 10°S.

What we have shown so far (e.g., the composite, the similarity between the standard deviation of ISO and interannual variability of the seasonal mean) are only indicative of a common mode of variability. To bring out the common spatial pattern of intraseasonal and interannual variability, the following procedure is adopted. An EOF analysis of the ISO-filtered 850-hPa winds from 1 June to 30 September for all 20 yr (1978–97) is carried out. The first EOF explaining 14.8% of the total intraseasonal variance and representing the dominant ISO mode is shown in Fig. 10a. The dominant interannual mode is obtained from an EOF analysis of seasonal mean (JJAS) 850-hPa winds for 40 yr (1958–97). The first EOF explaining 16.8% variance of interannual variability of the Indian summer monsoon is shown in Fig. 10b. That the interannual EOF1 represents dominant variability of the Indian summer monsoon is seen from the strong correlation between projection coeficient 1 (PC1) and IMR ($r = 0.62$) shown in Fig. 10c. The similarity between the dominant ISO mode and the dominant interannual mode is rather striking. The easterlies south of the equator, the cross-equatorial flow, the convergence of air mass from northwest and southwest over the Arabian Sea around 10°N, the monsoon trough, and the anticyclonic vortex around 75°E, 5°N are all common in both patterns. Therefore, a common spatial pattern governs both the ISOs and the interannual variability, thus linking the ISOs with the interannual variability of the Indian monsoon.

b. ISO activity and interannual variations of the seasonal mean

Although the ISOs may have a common mode of spatial variability with the interannual variations of the seasonal mean monsoon, they may not have appreciable influence on the latter unless the interannual variations of the ISO activity are significant. In this section, we estimate the amplitude of interannual variations of the ISO activity and compare it with the amplitude of interannual variability of the seasonal mean.

The standard deviation of ISO-filtered vorticity at 850 hPa and OLR between 1 June and 30 September is cal-

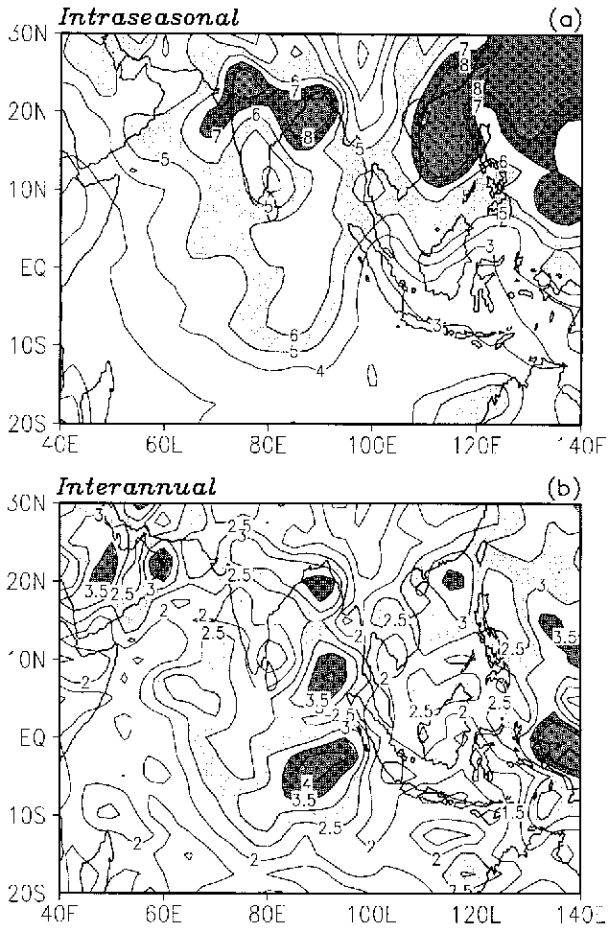

FIG. 9. Geographical distribution of intraseasonal and interannual activity. (a) Mean std dev of ISO-filtered relative vorticity (10^{-6} s^{-1}) at 850 hPa from 1 Jun to 30 Sep for 20 yr (1978–97). (b) Interannual std dev of seasonal mean relative vorticity (JJAS; 10^{-6} s^{-1}) based on the same 20 yr.

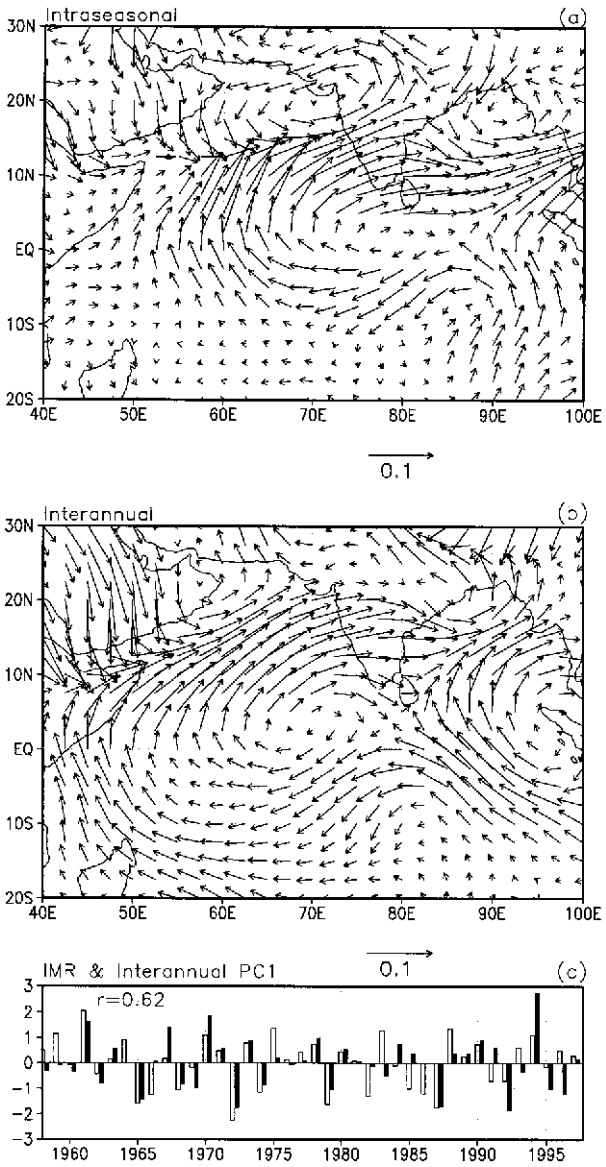

FIG. 10. First EOF of the intraseasonal and interannual 850-hPa winds. (a) Intraseasonal EOFs are calculated with ISO-filtered winds for the summer months (1 Jun–30 Sep) for a period of 20 yr (1978–97). (b) Interannual EOFs are calculated with the seasonal mean (JJAS) winds for 40-yr period (1958–97). Units of vector loading are arbitrary. (c) Relation between IMR and interannual PC1. Filled bars indicate interannual PC1, and the unfilled bars represent IMR. Both time series are normalized by their own standard deviation. Correlation between the two time series is shown.

culated each year at each grid point. The interannual standard deviation of this intraseasonal standard deviation of each year is calculated based on 20 yr (1978–97). The interannual standard deviation of seasonal mean vorticity at 850 hPa and OLR are separately calculated. The ratio between the standard deviation of interannual variations of ISO activity and interannual variation of seasonal mean is shown in Fig. 11. It is seen that magnitude and pattern of ratio is similar for both low-level vorticity and OLR. The equatorial belt (10°S–10°N) east of 100°E is characterized by a low ratio, as the interannual variations are stronger in this region. In most of the Indian monsoon regions, the ratio ranges from 0.4 to 0.8. This means that the variations of the ISO activity could account for 20%–60% of interannual variability of the seasonal mean in the Indian monsoon region. Thus, we can expect significant modulation of the seasonal mean monsoon by the ISOs.

c. Probability of occurrence of active/break conditions and seasonal mean monsoon

Because both the intraseasonal and interannual variations are associated with a common spatial pattern, a strong monsoon year should have a higher probability of occurrence of active conditions while a weak monsoon year should have a higher probability of occurrence of break conditions and a normal monsoon year should

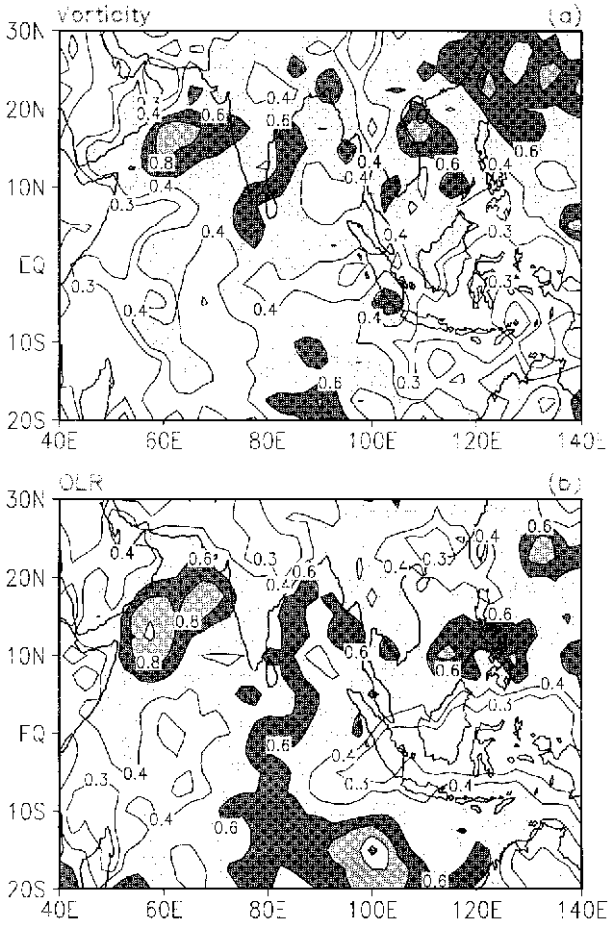

FIG. 11. Ratio between std dev of interannual variation of ISO activity and interannual variation of the seasonal mean. (a) Relative vorticity at 850 hPa. (b) OLR. Contours are 0.3, 0.4, 0.6, 0.8, 1.0.

have equal probability of occurrence of active and break conditions. This is essentially the same hypothesis proposed in our conceptual model (section 1). To test this hypothesis, we calculate probability density functions of the ISOs corresponding to strong and weak monsoon years. Strong and weak monsoon years are objectively defined based on whether IMR is greater than 1 standard deviation or less than -1 standard deviation. To have enough samples for such years, we use daily data between 1956 and 1997. This period contains 7 strong years (1956, 1959, 1961, 1970, 1975, 1983, 1988) and 10 weak monsoon years (1965, 1966, 1968, 1972, 1974, 1979, 1982, 1985, 1986, 1987). It may be noted here that the spatial pattern of the ISOs involve a northward propagating component. As a result, the evolutionary character of the active and break conditions cannot be described by a single EOF. To estimate the PDF of the ISOs, therefore, it is necessary to include more than one EOF. In the present study, we estimate the PDF of the ISOs using at least two EOFs. To obtain the PDF for the strong (weak) years, daily ISO-filtered 850-hPa vorticity between 1 June and 30 September for strong, weak, and "all" years (all 20 yr between 1978 and 1997 taken together) are combined, and an EOF analysis is carried out in each case using the singular value decomposition technique (Nigam and Shen 1993). The first two EOFs in each case are shown in Fig. 12. It may be noted that the first EOF in strong and weak cases for positive projection coefficients (PCs) represent activelike and breaklike conditions, respectively. The PDF of the PCs in the reduced phase space defined by the first two EOFs explaining 17% of the total variance of the strong years (21% for weak and 15% for all years) are obtained using a Guassian kernel estimator (Kimoto and Ghil 1993; Silverman 1986) with a smoothing parameter large enough to detect multimodality with statistical significance. The smoothing parameter (h) is selected from the minimum obtained from the least-squares cross-validation technique (Kimoto and Ghil 1993). In our case, h usually varies between 0.6 and 0.8. In these calculations, both the PCs are normalized by the temporal standard deviation of each of the PCs.

The two-dimensional PDF corresponding to strong, weak, and all years are shown in Figs. 13a, 13b, and 13c, respectively. For strong and weak years, the PDF of ISO activity is clearly non-Guassian, while in the case of all years, it is Guassian. The spatial pattern corresponding to the maxima of PDF in each case is constructed using appropriate normalization constants for the PCs and the corresponding EOF1 and EOF2 patterns. In the strong case, we note that the two maxima have almost equal probability. In the weak case, there are three maxima of the PDF patterns, while in the all case, there is only one maximum. As the number of strong and weak monsoon years included in the PDF calculation are quite large, we expect the maxima of PDFs in Figs. 13a and 13b to be robust. To test the statistical significance of these maxima, we created 1000 random sets of time series having the same variance and autocorrelation at 1-day lag equal to those of observed PC1 and PC2, and 2D PDFs were calculated for each of them. In Figs. 13a and 13b, shading represents regions where the observed PDF is significantly greater than the random ones with 90% confidence, that is, 25 or fewer of the random PDFs were larger than those shown in Figs. 13a and 13b. The maxima of the PDFs are found to be statistically significant in each case. In the strong and weak cases, we are primarily concerned with the statistical significance of the PDF maxima representing deviation from Guassian distribution. Since in the all case, the PDF pattern is Guassian, a similar significance test is not presented.

In the strong case, the maximum with normalized PC1 close to 1 and PC2 close to 0 represents a strong active condition shown in Fig. 14a. The other maximum represents a very weak break pattern. Although the two patterns have equal probability, strong active pattern would have the dominating influence on the seasonal mean. For the weak case, the maximum with both PC1 and PC2 close to 0 represents a transition pattern. Both

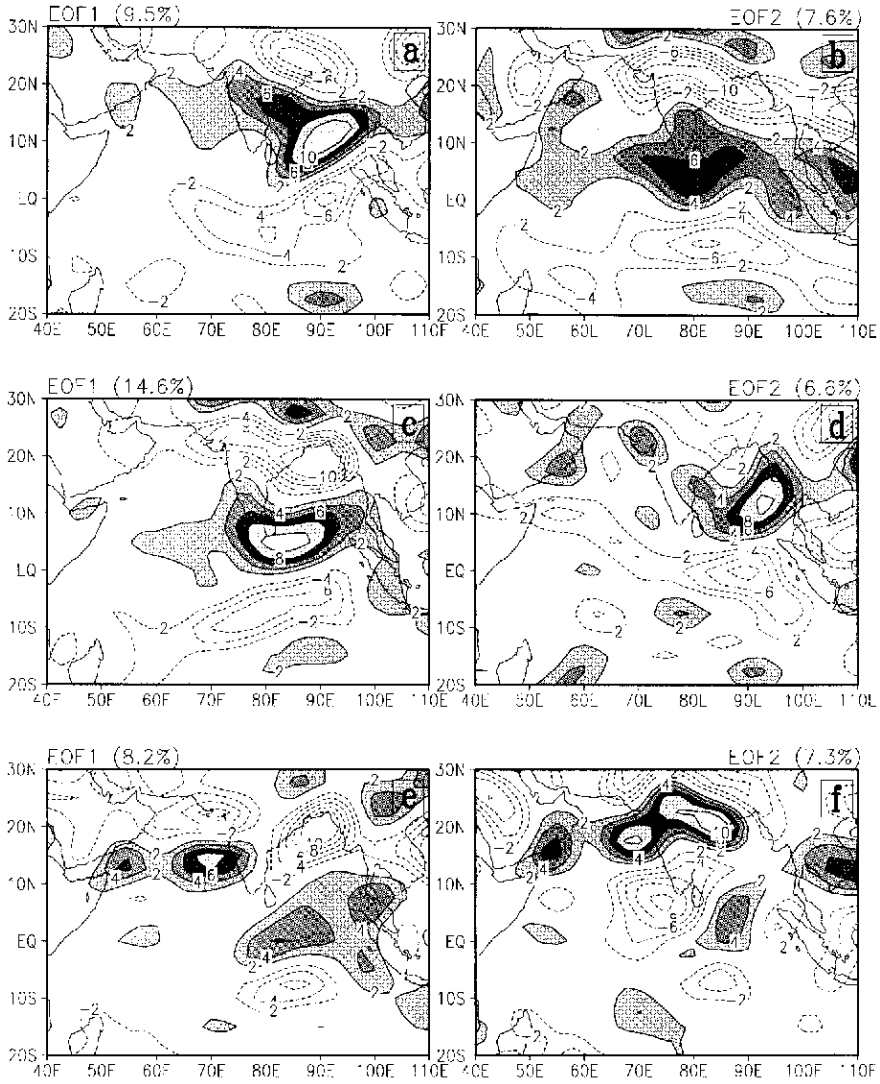

FIG. 12. First two EOFs of the daily ISO-filtered wind anomalies from 1 Jun to 30 Sep. (a) EOF1 and (b) EOF2 for 7 strong years; (c) EOF1 and (d) EOF2 for 10 weak years; (e) EOF1 and (f) EOF2 for all years (20 years from 1978 to 1997). Arbitrary EOF loadings have been multiplied by a factor of 100.

the other maxima represent strong break conditions. One such break condition with both PC1 and PC2 making approximately equal contributions is shown in Fig. 14b. On the other hand, the maximum of the PDF in the all year case corresponds to a transition pattern with insignificant vorticity associated with it, shown in Fig. 14c.

We note that the seasonal mean low-level vorticity over the northern TCZ position is cylclonic (see Fig. 1). The cumulative effect of a higher frequency of occurrence of active (break) conditions is expected to result in stronger (weaker) than normal cyclonic vorticity in this region. Since higher frequency of active (break) conditions are associated with strong (weak) Indian monsoon, we can expect a strong relationship between seasonal mean vorticity over the monsoon trough (northern position of TCZ) and the strength of the Indian monsoon. This conjecture is tested in Fig. 15, where we plot the seasonal mean relative vorticity averaged over the monsoon trough and IMR for the 40-yr period (1958–97). The correlation between the two time series is 0.74, strongly supporting our conjecture.

It would be desirable to see if the conclusions derived from circulation alone will be supported if convection is also included to describe ISOs. However, OLR data as proxy for convection is available only from 1974 onward. The period between 1974 and 1997 contains six weak monsoon years (1974, 1979, 1982, 1985, 1986, 1987), as described by the criterion used earlier. However, the same criterion indicates only three strong monsoon years in this period. To enhance the sample size

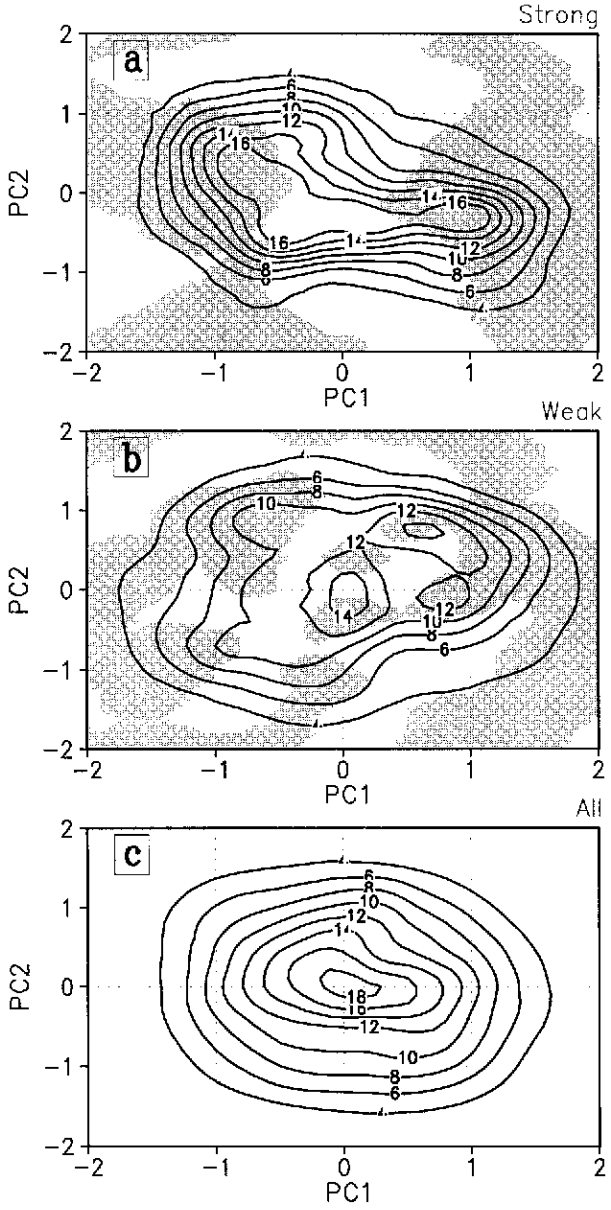

FIG. 13. Evidence of change in regimes of ISOs during strong and weak monsoon years. Illustrated are two-dimensional PDFs of the ISO state vector spanned by two dominant EOFs of low-level vorticity. The PDFs are calculated with principal components normalized by their own standard deviation and taking the summer days (1 Jun–30 Sep) for (a) 7 strong monsoon years, (b) 10 weak monsoon years, and (c) 20 combined strong, weak, and normal years (1978–97). The smoothing parameter used is $h = 0.6$, and PDFs are multiplied by a factor of 100. The first two EOFs (not shown) are different in strong, weak, and all years but are related to active and break conditions. The origin of the plots corresponds to a very weak state representing a transition between the two states (as in the all case).

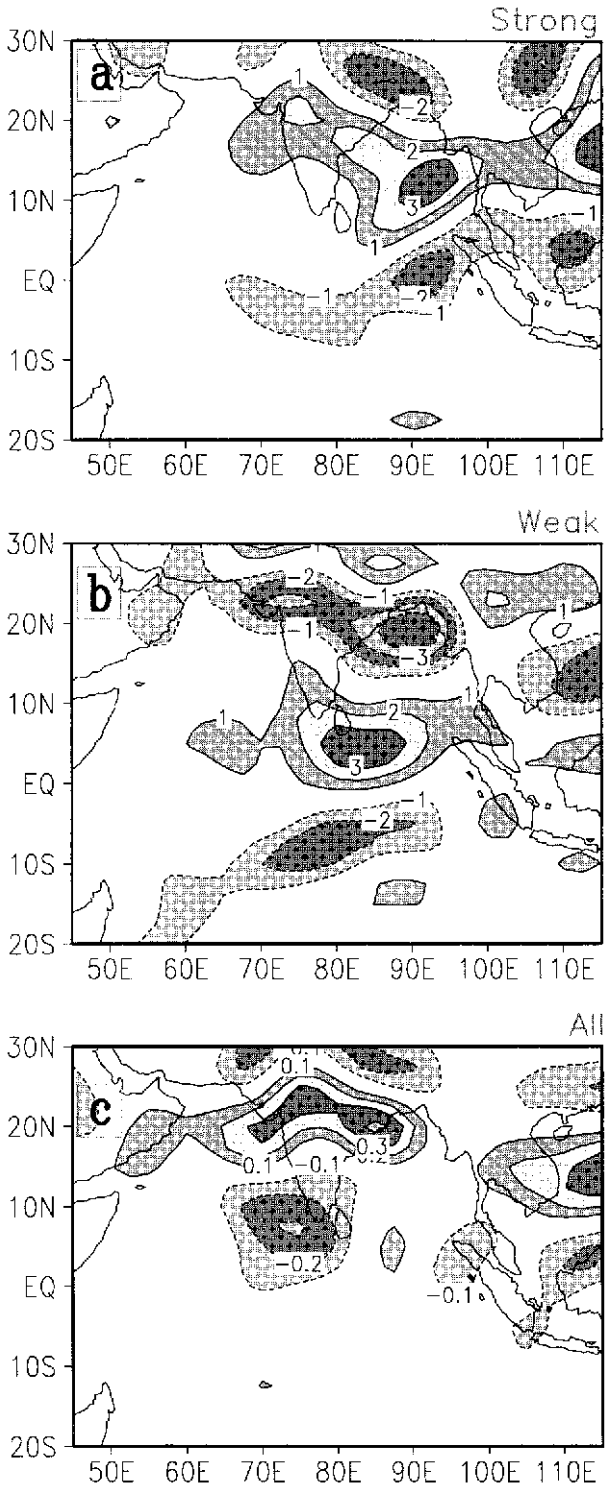

FIG. 14. Geographical patterns of the dominant regimes for low-level relative vorticity (10^{-6} s^{-1}) shown in Fig. 13. (a) Strong monsoon years, (b) weak monsoon years, (c) all years.

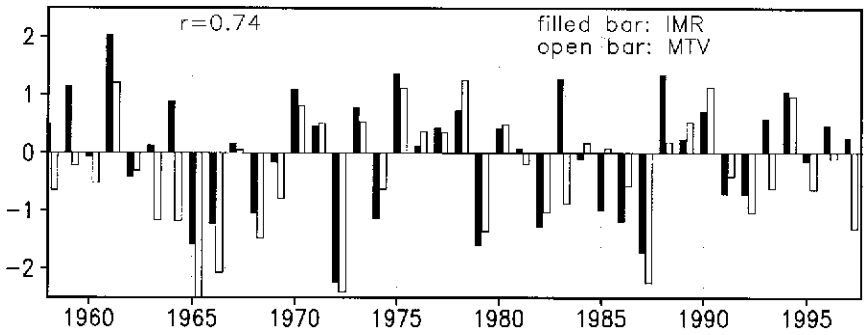

FIG. 15. The monsoon trough vorticity (MTV) and the IMR for a 40-yr period (1958–97). The MTV is defined as the seasonal mean vorticity (JJAS) averaged in the domain 40°–90°E and 10°–30°N. Both time series are normalized by their own standard deviation. Correlation between the two time series is shown.

of the strong monsoon years, we relaxed the objective criterion to include years for which IMR $>$ 0.5 std dev. Based on the relaxed criterion, six strong monsoon years (1975, 1978, 1983, 1988, 1990, 1994) are selected during this period. As in the previous case, a combined EOF (CEOF) analysis is carried out for 850 hPa vorticity and OLR for strong (weak) years. The PDF is then calculated on the reduced phase space defined by the first two EOFs. Similarly, the PDF of CEOF for all years (all 20 years from 1978–97) is also calculated. The PDFs for three different cases are shown in Fig. 16. It is clear that the PDFs are asymmetric for both strong and weak cases, while it is Guassian in the all case. As in the earlier case, statistical significance for the observed PDFs were carried out, and regions of phase space where the observed PDFs are significantly larger than the randomly generated ones with 90% confidence are shaded. Using appropriate normalization constants for the PCs and corresponding EOF1 and EOF2 (figure not shown), the patterns representing maxima in PDF are calculated. In the strong case, the most probable pattern corresponds to an active condition (Fig. 17a). The other maxima with much less probability represents a weak break condition (not shown). For the weak case, both maxima correspond to break conditions. The one with normalized PCs close to zero, however, represents a weak break condition (not shown), while the other maxima in PDF represent a strong break condition (Fig. 17b). The most probable pattern in the all case (Fig. 17c) corresponds to a very weak pattern representing a transition between active and break patterns.

5. Discussion and conclusions

The primary objective of this study is to investigate how and to what extent the monsoonal ISOs influence the seasonal mean and the interannual variability of the Indian summer monsoon. The underlying hypothesis is that the seasonal mean monsoon has a component forced by internal dynamics in addition to a component forced by external conditions. This hypothesis can be considered as an extension of the Charney and Shukla (1981) hypothesis, which suggested the interannual variation of Indian monsoon to be primarily forced by boundary forcing at the earth's surface. We propose that the part of the interannual variations of the seasonal mean that is independent of external forcing arises from the changes in the statistics of the intraseasonal oscillations of the Indian monsoon. Because the ISOs are intrinsically chaotic, the predictability of the seasonal mean Indian monsoon depends on the extent to which the ISOs influence the seasonal mean relative to the externally forced component. In the present study, we present a conceptual model to describe how the ISOs influence the seasonal monsoon. It envisages the ISO arising out of fluctuation of the tropical convergence zone (TCZ) between two favored regions, one over the monsoon trough (northern TCZ) and the other over the equatorial warm waters (southern TCZ). In one extreme of the ISOs (active phase), the TCZ resides over the northern position, strengthening the seasonal mean monsoon circulation, enhancing cyclonic vorticity over the northern TCZ, and enhancing convection (and precipitation) over that location while suppressing convection over the southern position. In the other extreme (break phase), weakened large-scale monsoon flow and weakened cyclonic vorticity over the northern position keeps the northern position clear of convection and helps enhance convection over the southern position. A higher probability of occurrence of active (break) conditions in a monsoon season results in a stronger (weaker) than normal seasonal mean monsoon. Thus, according to our conceptual model, the intraseasonal and interannual variations of the Indian monsoon are governed by a common mode of spatial variability. In addition, if indeed the ISOs determine the strong and weak monsoons, the PDF of the ISOs should have higher probability of occurrence of active conditions during strong monsoon years and break conditions during weak monsoon years. These two elements of our hypothesis are rigorously tested using a sufficiently long record of daily circulation and convection data.

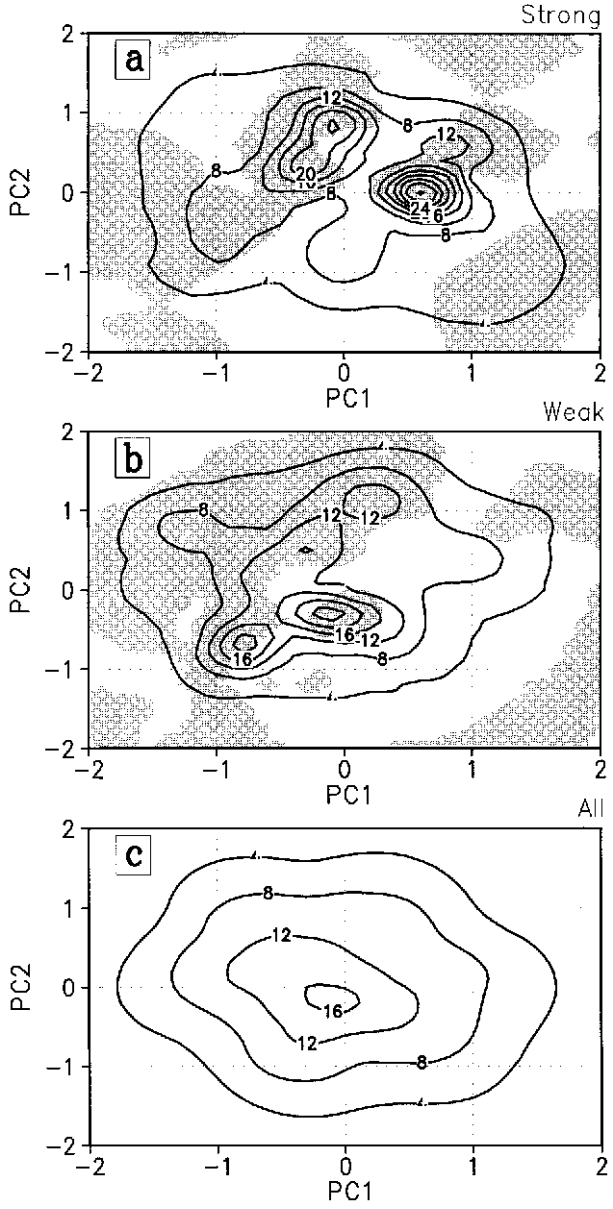

FIG. 16. Same as Fig. 13 but based on the state vector defined by the first two combined EOF of low-level vorticity and OLR.

In order to bring out the influence of the ISOs on the seasonal mean, it is desirable to separate the externally forced component of the seasonal mean from the internally forced component. We expect the slowly varying external forcing to give rise to slow and persistent changes and manifest in the interannual variation of the annual cycle. Intraseasonal anomalies are constructed in our study by removing the annual cycle of individual years (sum of annual and semiannual harmonics) from the observations. In this manner, we have been able to separate the influence of the external forcing on the ISOs. We believe that this procedure is important in bringing out the intrinsic role of the ISOs. Some studies define ISO anomalies with respect to climatological daily mean as an annual cycle, and hence the ISOs contain the effect of interannual variations of the annual cycle. This may be one reason why results of the previous studies have not been conclusive.

Our first objective was to find the mean large-scale spatial pattern associated with the ISOs and compare them with that of the seasonal mean pattern. For this purpose, we have evolved a "circulation" criterion for defining active and break monsoon conditions. Large-scale structure of the mean circulation anomalies associated with the active and break conditions of the dominant ISO modes are then obtained by constructing a composite of filtered 30–60-day or 10–20-day circulation anomalies at all points for all active and break days. A climatological mean of all such composites for individual years is then constructed, representing a spatial pattern of the active and break that is invariant from year to year. Such climatological mean composites corresponding to a typical active (break) condition of the 30–60-day mode are associated with a general strengthening (weakening) of the mean monsoon flow and strengthening (weakening) of the monsoon trough. It is rather interesting that the circulation changes are not confined only over the Indian region but extended all the way to the east of 120°E (South China Sea). The enhanced low-level cyclonic (anticyclonic) vorticity in the northern TCZ during an active (a break) condition is associated with enhanced (decreased) ascending motion leading to enhanced (decreased) convection over the northern TCZ and decreased (enhanced) ascending motion and decreased (enhanced) convection over the southern TCZ. In other words, the anomalous regional Hadley circulation has ascending motion over the northern TCZ and descending motion over the southern TCZ during an active condition, while the reverse is the case during a break condition. A typical evolutionary cycle of the dominant ISO based on composite of circulation and convection for 20 yr (1978–97) is also constructed and shows repeated northward propagation from the southern position to the northern position (monsoon trough).

The close resemblance between the spatial structure of the active and break composites and that of the seasonal mean indicate a similarity between the spatial structure of intraseasonal and interannual variability. The spatial distribution of standard deviation of 850-hPa vorticity associated with ISO variability and that of interannual variability of the seasonal mean are shown to be closely similar (pattern correlation 0.6; Fig. 9). That the intraseasonal and interannual variations are governed by a common spatial mode of variability is seen from the notable similarity between the dominant EOF of intraseasonal oscillations (based on 20 yr of daily ISO-filtered data during the summer season) and the dominant EOF of the interannual variation of the seasonal mean (based on 40 yr of seasonal mean data) (Fig. 10). In contrast to some recent studies (Annamalai

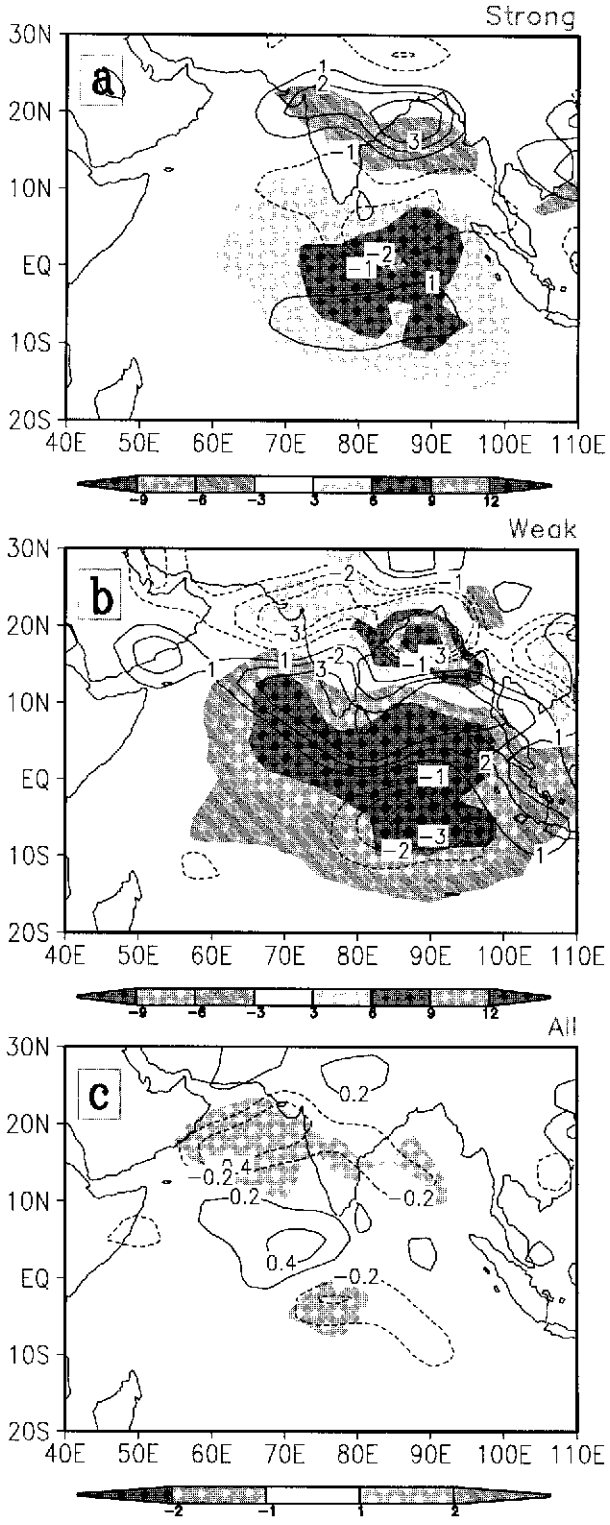

FIG. 17. Geographical patterns of the dominant regimes shown in Fig. 16. (a) Strong monsoon years, (b) weak monsoon years, (c) all years. OLR patterns are shown as shaded contours (W m^{-2}); the corresponding low-level vorticity is shown in contours (10^{-6} s^{-1}).

et al. 1999), where it is claimed that it is not possible to describe the interannual variations of the Indian summer monsoon by a single EOF, we show that the dominant EOF indeed represents interannual variations of the Indian summer monsoon (correlation between IMR and PC1 is 0.62) if the domain is restricted between 40°–100°E and 20°S–30°N. If the domain of analysis included regions east of 100°E, the ENSO-related variation in the eastern part of the domain dominates the first EOF, and the interannual monsoon variations may appear as the second EOF.

Next, we show that the interannual variations of the summer ISO variance has the potential for significantly influencing (up to 20%–60%) the interannual variations of the seasonal mean. Then, we argue that it is not the amplitude of the ISO activity but the asymmetry in the occurrence of the active and break conditions that affect the seasonal mean. We investigate whether the frequency of occurrence of active and break conditions is distinctly different during strong (flood years) and weak (drought years) monsoon years. For this purpose, a two-dimensional PDF estimate (Kimoto and Ghil 1993) is employed on the ISO-filtered field. A daily, low-level vorticity field between 1956 and 1997 is employed to include a large number of strong (7) and weak (10) monsoon years. This objective technique clearly shows that the PDFs are distinctly asymmetric and different during strong and weak monsoon years, and the most frequently occurring pattern during strong (weak) monsoon years is the active (break) pattern. On the other hand, if all years are linked together, the PDF is Guassian, with the transition between active and break patterns being the most frequently occurring pattern. Thus, the cumulative effect of the active condition during a strong monsoon season leads to stronger than normal cyclonic vorticity in the north TCZ position and stronger than normal seasonal mean. This conclusion is further supported by strong correlation between seasonal mean vorticity over the northern TCZ position and IMR (Fig. 15). That the conclusions arrived at from the PDF of low-level vorticity are robust is supported by the PDF estimate of combined low-level vorticity and convection. Using simultaneous convection and circulation data (1974–97), combined EOF of the low-level vorticity and OLR is carried out for all strong and weak years as well as all the years taken together. This calculation also shows that the most frequent pattern during a strong (weak) year is the active (break) pattern with enhanced (decreased) cyclonic vorticity and negative (positive) OLR anomaly over the northern TCZ position. Our results are consistent with recent findings of Krisnamurthy and Shukla (2000), where they examined daily rainfall over the Indian continent for the period 1901–70 and showed that strong (weak) monsoon years are associated with active (break) conditions (their Fig. 12a). They define ISO anomalies with respect to a climatological mean seasonal cycle. If they remove the "seasonal mean anomaly" (1 June–30 September) from

the anomalies, they do not find a clear signal of skewness in the PDF. This is understandable. Part of seasonal mean anomaly is due to the external forcing, but part is due to the ISOs themselves. If we remove the full seasonal mean anomaly from the data, all possible skewness of the PDF will be eliminated.

For the first time, we present unambiguous evidence from long records of observed daily circulation and convection data that shows that frequency of occurrence of active (break) conditions during a monsoon season determines the strength of the seasonal mean monsoon. All earlier studies either used a small sample size or used a methodology that was unable to separate the signal from the noise. This result has important implications in monsoon prediction itself. It indicates that the chaotic ISOs have strong influence on the seasonal mean monsoon. Hence, the prediction of the Indian monsoon is going to be difficult and would have to be probabilistic at best.

Acknowledgments. This work is supported in part by a grant from the Department of Science and Technology, Government of India. Comments by two anonymous reviewers on an earlier version of the manuscript are greatly appreciated and led to considerable improvement of the manuscript. We are grateful to Prof. M. Ghil, Dr. M. Kimoto, and Dr. A. Robertson for providing information regarding probability density estimation. We thank D. Sengupta for discussions and Mike Fennessy for providing the gridded daily rainfall data over India from 1971 to 1990. The authors are also grateful to Dr. U. S. De of India Meteorological Department for providing information on active/break conditions defined by IMD. The Super Computer Education and Research Center at the Indian Institute of Science, Bangalore, provided computing resources.

REFERENCES

Ahlquist, J., V. Mehta, A. Devanas, and T. Condo, 1990: Intraseasonal monsoon fluctuations seen through 25 years of Indian radiosonde observations. *Mausam,* **41,** 273–278.

Annamalai, H., J. M. Slingo, K. R. Sperber, and K. Hodges, 1999: The mean evolution and variability of the Asian summer monsoon: Comparison of ECMWF and NCEP–NCAR Reanalyses. *Mon. Wea. Rev.,* **127,** 1157–1186.

Charney, J. G., and J. Shukla, 1981: Predictability of monsoon. *Monsoon Dynamics,* J. Lighthill and R. P. Pearce, Eds., Cambridge University Press, 99–108.

Chatfield, C., 1980: *The Analysis of Time Series: An Introduction.* Chapman and Hall, 268 pp.

Dakshinamurthy, J., and R. N. Keshavamurthy, 1976: On oscillations of period around one month in the Indian summer monsoon. *Indian J. Meteor. Geophys.,* **27,** 201–203.

Fennessy, M., and J. Shukla, 1994: GCM simulations of active and break monsoon periods. *Proc. Int. Conf. on Monsoon Variability and Prediction,* Trieste, Italy, WMO/TD 619, WCRP-84, Vol. 2, 576–585.

Ferranti, L., J. M. Slingo, T. N. Palmer, and B. J. Hoskins, 1997: Relations between interannual and intraseasonal monsoon variability as diagnosed from AMIP integrations. *Quart. J. Roy. Meteor. Soc.,* **123,** 1323–1357.

Goswami, B. N., 1994: Dynamical predictability of seasonal monsoon rainfall: Problems and prospects. *Proc. Indian Nat. Sci. Acad.,* **60A,** 101–120.

——, 1997: Chaos and Predictability of the Indian summer monsoon. *Pramana,* **48,** 719–736.

——, 1998: Interannual variations of Indian summer monsoon in a GCM: External conditions versus internal feedback. *J. Climate,* **11,** 507–522.

——, and J. Shukla, 1984: Quasi-periodic oscillations in a symmetric general circulation model. *J. Atmos. Sci.,* **41,** 20–37.

——, D. Sengupta, and G. Suresh Kumar, 1998: Intraseasonal oscillations and interannual variability of surface winds over the Indian monsoon region. *Proc. Indian Acad., Sci., Earth Planet. Sci.,* **107,** 45–64.

Gruber, A., and F. Krueger, 1984: The status of NOAA outgoing longwave radiation data set. *Bull. Amer. Meteor. Soc.,* **65,** 958–962.

Hartman, D. L., and M. L. Michelson, 1989: Intraseasonal periodicities in Indian rainfall. *J. Atmos. Sci.,* **46,** 2838–2862.

Harzallah, A., and R. Sadourny, 1995: Internal versus SST forced atmospheric variability simulated by an atmospheric general circulation model. *J. Climate,* **8,** 474–495.

Kalnay, E., and Coauthors, 1996: The NCEP/NCAR 40-Year Reanalysis Project. *Bull. Amer. Meteor. Soc.,* **77,** 437–471.

Keshavamurthy, R. N., 1973: Power spectra of large scale disturbances of the Indian south-west monsoon. *Indian J. Meteor. Geophys.,* **24,** 117–124.

——, S. V. Kasture, and V. Krishnakumar, 1986: 30–50 day oscillation of the monsoon: A new theory. *Beitr. Phys. Atmos.,* **59,** 443–454.

Kimoto, M., and M. Ghil, 1993: Multiple flow regimes in the northern hemisphere winter. Part I: Methodology and hemispheric regimes. *J. Atmos. Sci.,* **50,** 2625–2643.

Krishnamurti, T. N., and H. N. Bhalme, 1976: Oscillations of monsoon system. Part I. Observational aspects. *J. Atmos. Sci.,* **33,** 1937–1954.

——, and P. Ardunay, 1980: The 10 to 20 day westward propagating mode and ''breaks in the monsoons.'' *Tellus,* **32,** 15–26.

——, and D. Subrahmanyam, 1982: The 30–50 day mode at 850mb during MONEX. *J. Atmos. Sci.,* **39,** 2088–2095.

Krishnamurthy, V., and J. Shukla, 2000: Intraseasonal and interannual variability of rainfall over India. *J. Climate,* **13,** 4366–4377.

Mehta, V. M., and T. N. Krishnamurti, 1988: Interannual variability of 30–50 day wave motion. *J. Meteor. Soc. Japan,* **66,** 535–548.

Murakami, M., 1979: Large scale aspects of deep convective activity over the GATE area. *Mon. Wea. Rev.,* **107,** 994–1013.

Murakami, T., and T. Nakazawa, 1985: Tropical 45 day oscillations during 1979 Northern Hemisphere summer. *J. Atmos. Sci.,* **42,** 1107–1122.

——, ——, and J. He, 1984: On the 40–50 day oscillation during 1979 Northern Hemisphere summer. Part 1: Phase propagation. *J. Meteor. Soc. Japan,* **62,** 440–468.

Nigam, S., and H. S. Shen, 1993: Structure of oceanic and atmospheric low-frequency variability over the tropical Pacific and Indian Oceans. Part I: COADS observations. *J. Climate,* **6,** 657–676.

Palmer, T. N., 1994: Chaos and the predictability in forecasting monsoons. *Proc. Indian Nat. Sci. Acad.,* **60A,** 57–66.

Parthasarathy, B., A. A. Munot, and D. R. Kothawale, 1994: All India monthly and seasonal rainfall series: 1871–1993. *Theor. Appl. Climate,* **49,** 217–224.

Ramamurthy, K., 1969: Monsoon of India: Some aspects of 'break' in the Indian south west monsoon during July and August. Forecasting Manual, Report IV, Vol. 18. [Available from India Meteorological Department, Pune–411005, India.]

Rowell, D., C. K. Folland, K. Maskell and M. N. Ward, 1995: Variability of summer rainfall over tropical north Africa (1906–1992): Observations and modelling. *Quart. J. Roy. Meteor. Soc.,* **121,** 669–704.

Salby, M., H. Hudson, K. Woodberry, and K. Tavaka, 1991: Analysis

of global cloud imagery from multiple satellites. *Bull. Amer. Meteor. Soc.,* **72,** 467–479.

Sikka, D. R., and S. Gadgil, 1980: On the maximum cloud zone and the ITCZ over Indian longitudes during the southwest monsoon. *Mon. Wea. Rev.,* **108,** 1840–1853.

Silverman, B. W., 1986: *Density Estimation for Statistics and Data Analysis.* Chapman and Hall, 174 pp.

Singh, S. V., and R. H. Kripalani, 1990: Low frequency intraseasonal oscillations in Indian rainfall and outgoing long wave radiation. *Mausam,* **41,** 217–222.

——, ——, and D. R. Sikka, 1992: Interannual variability of the Madden-Julian oscillation in the Indian summer monsoon rainfall. *J. Climate,* **5,** 973–978.

Stern, W., and K. Miyakoda, 1995: The feasibility of seasonal forecasts inferred from multiple GCM simulation. *J. Climate,* **8,** 1071–1085.

Webster, P. J., 1983: Mechanism of monsoon low-frequency variability: Surface hydrological effects. *J. Atmos. Sci.,* **40,** 2110–2124.

——, V. O. Magana, T. N. Palmer, J. Shukla, R. T. Tomas, M. Yanai, and T. Yasunari, 1998: Monsoons: Processes, predictability, and the prospects for prediction. *J. Geophys. Res.,* **103(C7),** 14 451–14 510.

Xie, P., and P. Arkin, 1996: Analyses of global monthly precipitation using gauge observations, satellite estimates, and numerical model predictions. *J. Climate,* **9,** 840–858.

Yasunari, T., 1979: Cloudiness fluctuation associated with the Northern Hemisphere summer monsoon. *J. Meteor. Soc. Japan,* **57,** 227–242.

——, 1980: A quasi-stationary appearance of 30–40 day period in the cloudiness fluctuation during summer monsoon over India. *J. Meteor. Soc. Japan,* **58,** 225–229.

——, 1981: Structure of an Indian summer monsoon system with around 40-day period. *J. Meteor. Soc. Japan,* **59,** 336–354.